LIP-STUDENTS-EXT-25-04

Optical characterization of novel plastic scintillators for future detectors

Gonçalo Rosa[1,a]

[1] *Instituto Superior Técnico, Lisboa, Portugal*

Project supervisor: R. Pedro, A. Gomes

October 9, 2025

Abstract. This report outlines the development and commissioning of an experimental setup for characterizing the dominant scintillation time properties of Polyethylene Terephthalate (PET), Polyethylene Naphthalate (PEN) and PET:PEN mixture scintillators for high-energy particle detection. The fundamental principles of organic scintillation are described, and an appropriate setup is presented for analyzing multiple scintillation characteristics that are cross-referenced with literature and used as probes for data and setup quality. Multiple results are shown, both for confirming the validity of the experiment as well as presenting new data for the use of these novel plastic scintillators, specifically their potential use in extreme rate experiments such as those in the High Luminosity Large Hadron Collider (HL-LHC) and/or Future Circular hadron Collider (FCC-hh).

Keywords: Plastic scintillators, Decay Time, Polyethylene Naphthalate, Polyethylene Terephthalate

1 Introduction

1.1 Motivation

A scintillator is a material that emits light when excited by ionizing radiation. PEN and PET plastics, which are most commonly used in polyester fibers and commercial packaging of food products [1, 2], have shown themselves as possible competitor materials for scintillation detection. However, the use of these plastic compounds is still new and requires extensive analysis of their properties, such as light response, scintillation decay time constants, and radiation resistance, to name a few. The data that already exists on these properties will be used as cross-references to validate our setup and method [3-5]. Although the use of PEN and PET as scintillators is a new development, the physics of plastic scintillators has been understood for quite some time [6], and they have been used in various experiments. Given the size and scope of large detectors in future collider experiments, PEN and PET are a promising low-cost alternative [7].

In extreme rate collision experiments, it is essential that scintillators emit the dominant component of their total light response in a similarly short time period. For reference, the LHC has a collision rate corresponding to 1 bunch crossing per 25 ns [8]. The decay constant (τ) is defined as the average time it takes for a scintillator to reach $1/e$ of its initial light emission peak, which can be modeled by:

$$I = I_0 \cdot \mathrm{e}^{-t/\tau} \tag{1}$$

for organic fluorescent materials [9].

1.2 Materials properties

Both PEN and PET plastics are composed of aromatic molecules, which make their scintillation properties possible. The mechanism for their absorption of energy and subsequent emission originates in the presence of double-bonded hydrocarbons along the benzene ring structure.

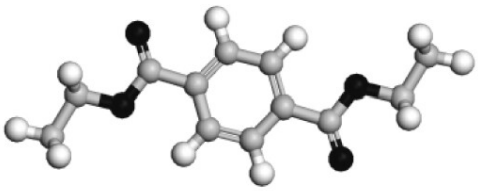

Figure 1. Diethyl Terephthalate, the main molecule of PET, from [10].

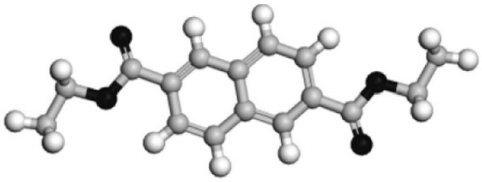

Figure 2. Dimethyl 2,6-Naphthalene Dicarboxylate, the main molecule of PEN, from [10].

Given the C_6 atoms compound forming orbital distribution of $1s^1 2s 2p^3$, where one of the $2s$ electrons occupies a $2p$ orbital for bonding, in the case of a double-bonded hydrocarbon there is sp^2 hybridization where one of the $2p$ orbitals is left unchanged and the remainder combine to form a planar structure. This "free" $2p$ orbital and electrons are named π-orbitals and π-electrons respectively. When paired with other trigonal hydrocarbons, these "free" π orbitals are able to interact with each other and give rise to what we call "double-bonds". It's the excitation of these π-orbital configurations that allows the mechanism of luminescence to occur in these molecules. Looking at the structure of the individual molecules that compose PET and PEN, Fig. 1 and Fig. 2, we can observe that these display the characteristics we are looking for in scintillation material.

[a] e-mail: goncalo.m.p.rosa@tecnico.ulisboa.pt

These π-orbitals allow for different energy states of free electrons within the molecule, which in turn can be excited by high-energy particles passing through the material and transferring their energy [9]. However, this process can be affected by multiple quenching phenomena, which can alter the amount of light emitted and the efficiency of the material as a scintillator, both in long-term use and single emission events. There is also the common presence of slow-emission phenomena in organic scintillators, which have multiple interpretations and theories behind their origin and will be accounted for in later analysis [11]. We will now shift focus to the timing characteristics of the scintillation phenomena, alongside detailing the experiment to measure those.

2 Experimental Setup

2.1 Trigger and test scintillators

Each scintillation event is an inherently statistical phenomenon where shortly after being hit by ionizing radiation, the molecule can decay in various forms, with the statistical average of this emission timing following an exponential distribution with a well-defined decay constant. Therefore, to characterize this time dependency, it is necessary to stimulate the sample with a radiation source, acquire multiple scintillation events, and record their average timing given a well-known trigger in sync with the emission of the excitation source. In order to achieve this, we will use an experimental setup with two different scintillators, one of which will serve simply as an acquisition trigger, and the other will be the sample to test.

The different material samples for testing were developed at the Institute for Polymers and Composites at the University of Minho and were made as a double 30×30 mm^2 squares with a thickness of 2 mm. Fig. 3 shows the original injected samples, which were then cut individually from the support and polished on the sides for better optical coupling with the photo-detector [12]. From the different types produced, we will focus our analysis on the pure PEN and PET samples, the 50% PEN and 50% PET mixture (50:50), the 75% PEN and 25% PET mixture (75:25) and the 90% PEN and 10% PET mixture (90:10). It will also be common to represent graphical data as a function of percentage of PEN content (0%, 50%, 75%, 90% and 100% PEN). Multiple samples of the same material were made, and each is assigned a unique sample number (e.g., PET13).

2.2 Setup

These samples were measured in the setup represented in Fig. 4. A collimated Sr-90 radioactive source emits β^- particles in the vertical direction up to the location of the sample. However, in order to reach the sample, the particle must first pass through a group of scintillating fibers with a very well-known and quick time decay constant ($2-3$ ns), which are connected to a photo-multiplier (PMT) and will act as a trigger signal for an oscilloscope to record the data.

Figure 3. Samples excited by UV light, taken from [13].

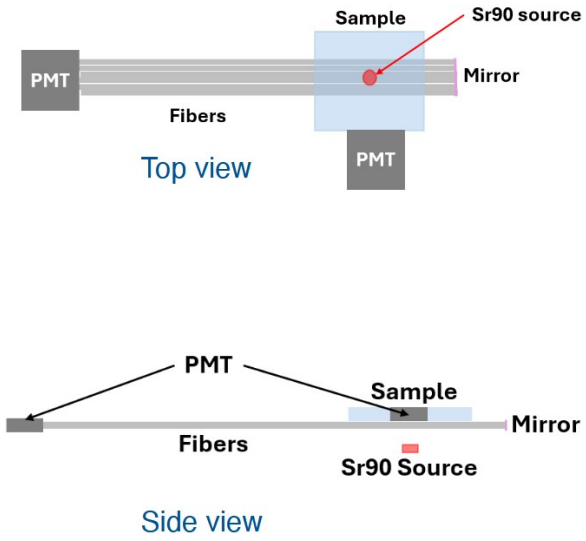

Figure 4. Experimental Setup sketch.

Between the fibers and the sample is a layer of Tyvek® sheet to prevent light cross-talk from both sides, allowing the particle to pass but not the emitted light. The particle now passes through and interacts with the sample, causing a scintillation phenomenon, and the light that the sample emits is captured by a second PMT directly coupled to the sample side. The PMT then transmits the electrical signal to the triggered oscilloscope, and the data for a single scintillation event is recorded.

This oscilloscope works with 10 GHz sampling, meaning that we have a time resolution of 0.1 ns for each event. Each event is recorded in a 250 ns time window that starts at -30 ns and ends at 219.9 ns. The PMTs themselves have a 0.2 ns transit time spread, meaning that we have confidence that the setup itself isn't introducing a substantial amount of uncertainty and that the time profile of the light pulse isn't deformed when transiting into an electric signal.

A single recorded event is expected to have somewhat randomly distributed peaks from secondary decays and molecule excitation phenomena [11]. These singular events will be recorded in 5 sets of one-hour runs for each sample type and exported as CSV files containing

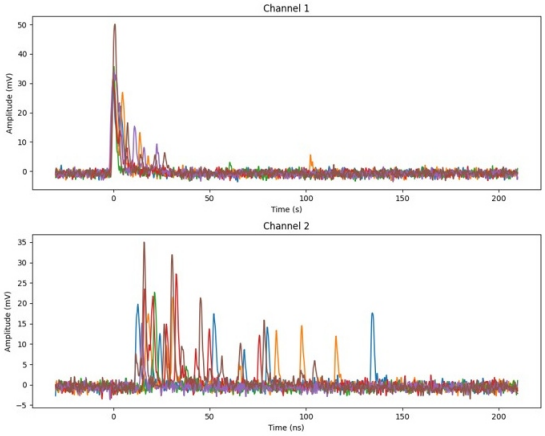

Figure 5. Graphical representation of a 6-event data set.

the data for all events bundled together, one file containing the trigger data and the other the sample data. The data itself consists of a matrix where the first column contains the corresponding time bin, and the others contain the recorded value of the amplitude at that time. The fibers' PMT is supplied −850 V by a high voltage supplier, and the sample PMT is supplied $-950V$, given that the light response of the fiber is expected to be much stronger. The experiment itself is contained within a light-tight dark box that shields the setup from any external light and allows the PMTs to function with such high power without fear of over-saturation. The fiber data is given an amplitude acquisition threshold of 30 mV while the sample data is given a varying threshold depending on the acquisition year and sample type.

3 Analysis

3.1 Data processing

In order to know whether our results are valid or not, we will take time to analyze and confirm various measured properties for both PEN and PET samples. Singular event acquisitions, like the one represented in Fig. 5, are very insufficient for getting general ideas of the scintillators' and experiment function, much less any numerical results, so the CSV files containing the data were processed through Python code using the Pandas and MatPlotLib libraries to represent data in multiple graphs and compute or extract numerical quantities for each data set.

Before any method can be used, the data is corrected and adjusted based on the analysis threshold parameters. The first step involves suppressing the non-zero value of the pulse pedestal, where, on average, for a time window with no possible events, the standard value of the oscilloscope acquisition was found to be around −1 mV. To determine the pedestal, we take advantage of the fact that the oscilloscope records around 30 ns of noise before the rise of the trigger pulse, given that the chance for an emission is incredibly low during this time. We take the average value of the amplitude during this interval and subtract it from the data set. This ensures that the integral sum of the pulse amplitudes over time will be positive and assists the fit function to more accurately approximate over the "close to zero" parts of the data set. We also analyze data for various amplitude thresholds of the sample pulse to study the effect that different thresholds may have on the results.

3.2 Data analysis

The analysis of data to determine the scintillation decay constant will rely on two different methods, the Average Amplitude method (AA) and the Time Differences method (TD). The AA method involves averaging the amplitude of each time interval bin over the acquired pulses and fitting a decay function over the resulting graph. The TD method, in turn, takes the first peak of each event over the given threshold and plots the time difference between the fiber peak and the sample peak, resulting in a time difference distribution, which is then fitted with an exponential decay function. While we expect similar results from these two methods, there is a very important nuance: while the AA method incorporates every event's secondary emissions, and thus the slow component of the luminescence phenomenon, the TD method only uses the quickest peak over amplitude threshold, and is not sensitive to slower secondary emissions. Therefore, we will use two different functions for the fitting, the TD function will be a single exponential similar to the one we referenced in literature (Eq. 1):

$$I = I_0 \cdot \mathrm{e}^{-t/\tau} \tag{2}$$

while the AA method will use a double exponential to take into account the slow component:

$$A(t) = A_f \cdot \mathrm{e}^{-t/\tau_f} + A_s \cdot \mathrm{e}^{-t/\tau_s} \tag{3}$$

put under the condition that $\tau_f < \tau_s$. There is also a single exponential fit made for the AA method, which seeks to capture the dominant time decay component and compare with the TD method results.

Each sample data set is exported with both visual graphics data as well as numerical data points for ease of comparison between different samples. Fig. 6 shows the exported graph for AA with the blue line showing the down-scaled average fiber data, the yellow line representing the average values of the amplitudes of the scintillator sample pulses with the standard deviation in clear transparent yellow, and the red line representing the double exponential fit. Fig. 7 shows the distribution of the time interval between the fiber and the sample pulses obtained with the TD method, together with the simple exponential fit. The AA single exponent fit, a fiber data fit, and a histogram of event peak amplitudes are also produced, but they are more relevant as numerical data than as visual representations, so they will not be shown here.

4 Results

After acquiring and analyzing data from various samples, we found multiple results that indicate that the experiment

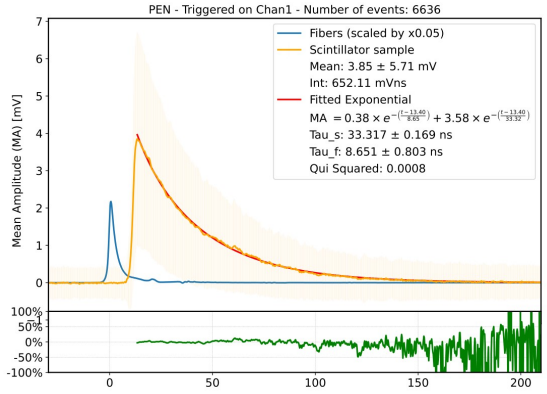

Figure 6. Analysis Graph of PEN25 using AA.

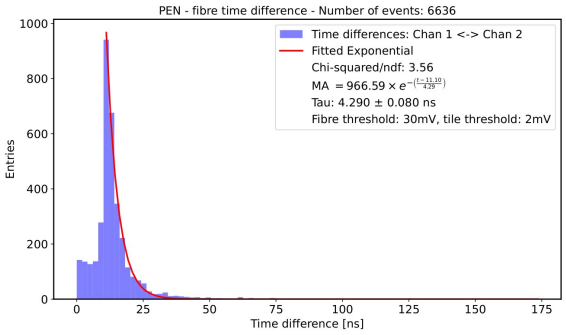

Figure 7. Analysis Graph of PEN25 using TD.

can successfully determine the decay constant. These results will most commonly be divided into the 2024 data acquisition set and the 2025 set, where only slight alterations to the setup and high voltage supply were made. The same samples were measured in both years to check the reliability of the setup.

To characterize the experimental background, several acquisitions were made with the Sr-90 source moved out of the setup's trajectory, resulting in a detection rate of around 61 ± 9 events per hour. The rate of cosmic muons that reach the surface of the Earth is around 60 particles per square centimeter per hour [14]. Given that the area of the detector, as in the area in which the fibers and sample overlap, is 0.9 cm^2, we should be seeing a rate of 54 background events per hour originating from cosmic muons, which is compatible with our results.

Given the ability to probe the light intensity response based on the measured average pulse integral using the AA method, we can verify that the light emitted from PEN is around 5 – 7 times that of PET, which is corroborated by the literature [13]. Fig. 8 shows the integral as a function of PEN proportion, which, despite a clear lack of precision from the setup, still gives accurate enough data to verify this point.

Fiber data was also analyzed in conjunction with every data run and was found to be qualitatively consistent in terms of light response, which is much larger than the

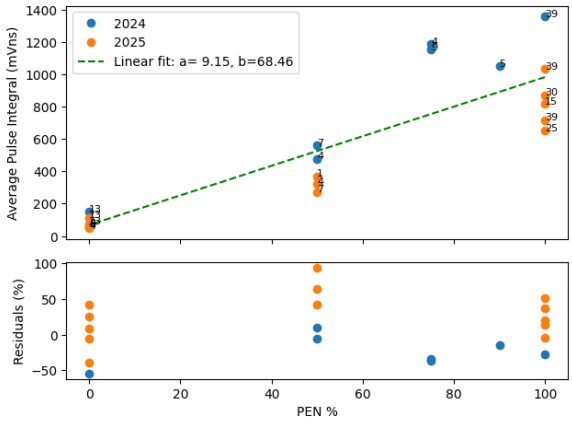

Figure 8. AA Average Pulse Integral as a function of PEN proportion.

samples'. The fiber decay constant result, for which the average of all runs gave $\tau = (3.0 \pm 0.1)$ ns, is compatible with the decay constant value range given by the manufacturer, and has also a very low spread in time decay values.

Given the small number of runs with samples 75:25 and 90:10, these will be omitted from the data table. We will present the results of both the TD fit (τ_{TD}), the AA double exponential fit (τ_{AAf} and τ_{AAs})[1], and the AA single exponential fit ($\tau_{AA\text{single}}$).

The decay constants determined with the AA method are shown in Fig. 9 and Fig. 10, and the relative dominance of each component is shown in Fig. 11 and Fig. 12. Both have the respective sample number next to the corresponding data point. In addition, the time decay results obtained with the TD method are also displayed in Fig. 13. A more detailed analysis of these results allows us to conclude the following:

- For PET samples, the fast amplitude determined with the AA analysis is around 90%, meaning that the dominant light emission is fast with an exponential decay constant of around 4 ns. The results are compatible with what is obtained from the simple exponential fit to the TD histogram.
- For PEN samples, the slow amplitude from the AA double exponential fit is between 80 to 90%, meaning that dominant light emission is slower and most probably associated with multiple quenching effects, well described by an exponential decay constant of around 35 ns. The TD analysis, sensitive to the sub-dominant fast emission, constrains the fast decay time constant poorly, as is also the case for the AA method.
- For mixture samples, the scintillation time properties are similar to PEN, which is justified by PEN having a much larger light yield than PET.

[1] The τ_{AAf} and τ_{AAs} represent the fast and slow time decay constants of the exponential fit obtained with the AA method, respectively.

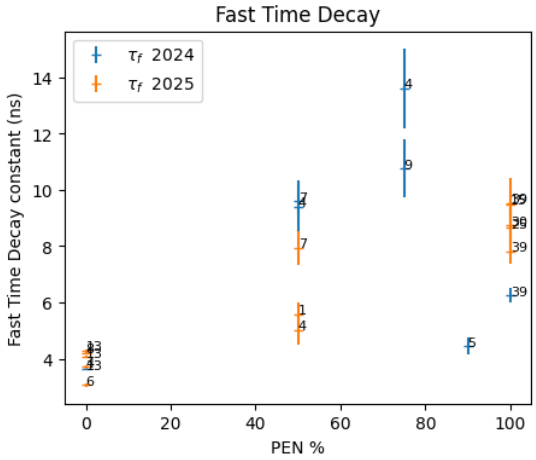

Figure 9. AA Fast Time Decay Constant as a function of PEN proportion.

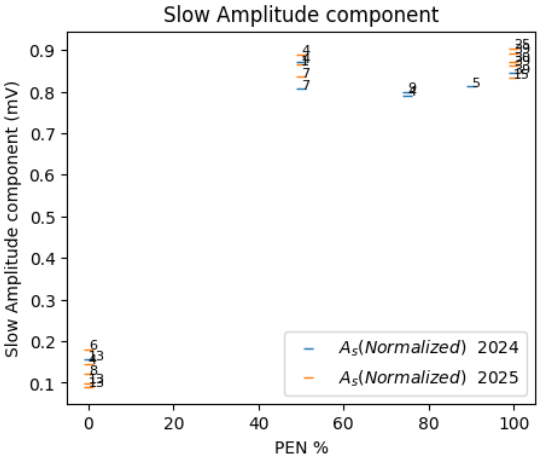

Figure 12. AA Slow Amplitude Components as a function of PEN proportion.

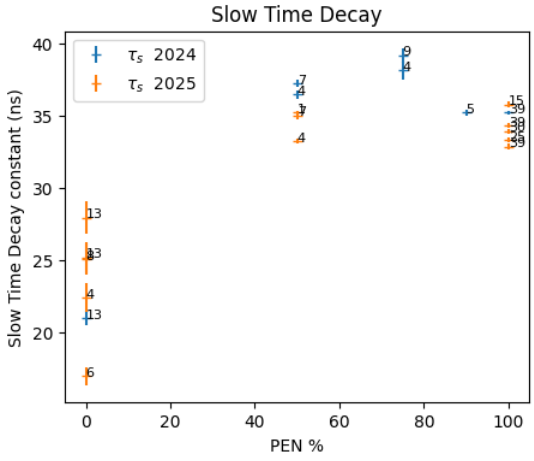

Figure 10. AA Slow Decay Time Constant as a function of PEN proportion.

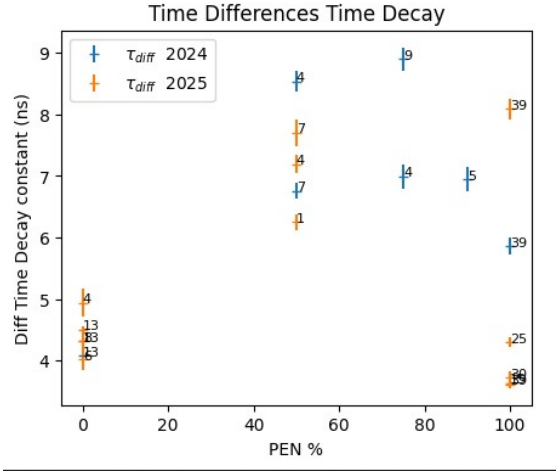

Figure 13. TD Decay Time Constant as a function of PEN proportion.

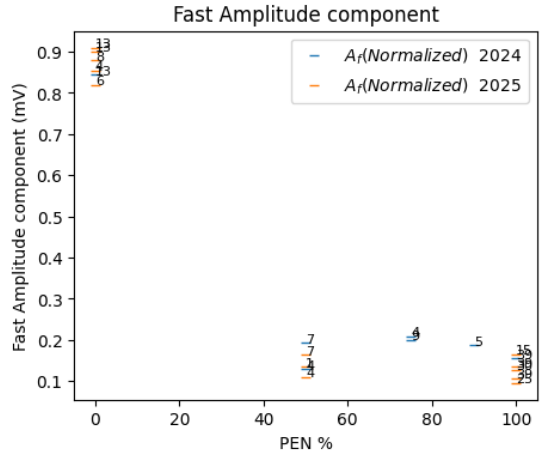

Figure 11. AA Fast Amplitude Components as a function of PEN proportion.

Sample	PEN	50:50	PET
τ_{TD}	4.9 ± 1.6	7.3 ± 0.8	4.4 ± 0.3
τ_{AAf}	8.1 ± 1.7	7.5 ± 1.9	3.8 ± 0.4
τ_{AAs}	34.3 ± 1.0	35.4 ± 1.4	23.1 ± 3.5
$\tau_{AAsingle}$	31.9 ± 0.6	32.8 ± 0.8	5.5 ± 0.3

Table 1. Average decay time constants, in ns, for the PEN, 50:50 and PET samples.

These results are summarized per sample material in Table 1, showing the average time decay over the different samples of the same material and the corresponding standard deviation given by the root of the unbiased sample variance. Results from a single exponential function fitted to the AA method are also shown.

Both the PEN and PET average results are in agreement with the literature, reporting dominant decay constants of 35 and 7 ns, respectively [5]. Given that the standard deviation is much larger on the non-dominant decay constant, which, for that reason, is prone to a less precise determination, we have confidence in these results.

The TD and AA methods give similar results for the fast components of the scintillation for all samples, which is expected, given the TD method's insensitivity to secondary (slower) emission components. It is noticed that the simple exponential fit resulting from the AA method captures the dominant time characteristic of the emission, with the obtained decay constant being similar to the fast constant for PET and to the slow constant for PEN.

5 Conclusion

Despite possible variations between different samples of the same type, we can confidently say the experiment has the potential to give accurate results for the decay constant of plastic scintillator samples and is a promising start for the acquisition of more data regarding this subject. However, there are still improvements and tests that can be made, such as the measurement of a well-known scintillating crystal, as well as more data sampling throughout the year to rule out any possible dependency on external factors.

6 Acknowledgments

I'd like to thank my supervisor Rute Pedro for the consistent and extremely helpful guidance within both the laboratory and the project as a whole, supervisor Agostinho Gomes for coordinating the LOMaC laboratory and giving me the opportunity to work with them, Rudnei Machado, João Gentil, Luís Gurriana and the whole LIP and LOMaC teams for allowing me to work besides them and learn from their vast experience. Thank you.

References

[1] J. Whinfield, Textile Research Journal **23**, 289 (1953), https://doi.org/10.1177/004051755302300503

[2] P.R. Ashurst, R. Hargitt, in *Soft Drink and Fruit Juice Problems Solved*, edited by P.R. Ashurst, R. Hargitt (Woodhead Publishing, 2009), Woodhead Publishing Series in Food Science, Technology and Nutrition, pp. 117–131, ISBN 978-1-84569-326-8, https://www.sciencedirect.com/science/article/pii/B9781845693268500050

[3] H.K. H. Nakamura, R. Hazama, Proceedings of the Royal Society A: Mathematical, Physical and Engineering Sciences **466**, 2847–2856 (2010)

[4] H. Nakamura, Y. Shirakawa, S. Takahashi, H. Shimizu, Europhysics Letters **95**, 22001 (2011)

[5] E.B.B.B.N. WETZEL, JAMES; TIRAŞ, O.K. KÖSEYAN, Turkish Journal of Physics **44** (2020)

[6] J. BIRKS, in *The Theory and Practice of Scintillation Counting*, edited by J. BIRKS (Pergamon, 1964), International Series of Monographs in Electronics and Instrumentation, pp. 321–353, ISBN 978-0-08-010472-0, https://www.sciencedirect.com/science/article/pii/B9780080104720500148

[7] A. et al (ATLASTileCal), Tech. rep., CERN, Geneva (2007), this note written by IHEP Group, Protvino., https://cds.cern.ch/record/1075711

[8] I.Z.F. et al in, *High-Luminosity Large Hadron Collider (HL-LHC): Technical design report*, CERN Yellow Reports: Monographs (CERN, Geneva, 2020), https://cds.cern.ch/record/2749422

[9] J. BIRKS, in *The Theory and Practice of Scintillation Counting*, edited by J. BIRKS (Pergamon, 1964), International Series of Monographs in Electronics and Instrumentation, pp. 39–67, ISBN 978-0-08-010472-0, https://www.sciencedirect.com/science/article/pii/B9780080104720500082

[10] A. Espinoza-Martínez, C. Avila-Orta, V. Cruz-Delgado, O. Olvera-Neria, J. González-Torres, F. Medellín-Rodríguez, Journal of Nanomaterials **2012**, 189820 (2012), https://onlinelibrary.wiley.com/doi/pdf/10.1155/2012/189820

[11] J. BIRKS, in *The Theory and Practice of Scintillation Counting*, edited by J. BIRKS (Pergamon, 1964), International Series of Monographs in Electronics and Instrumentation, pp. 185–234, ISBN 978-0-08-010472-0, https://www.sciencedirect.com/science/article/pii/B9780080104720500112

[12] P.M. R. Pedro, *New plastic scintillators for future light-based detectors, https://www.lip.pt/files/training/papers/2022/pdf/lip-students-22-26-lomac.pdf (accessed 26/06/2025)*, https://www.lip.pt/files/training/papers/2022/pdf/LIP-STUDENTS-22-26-Lomac.pdf

[13] P. Conde Muíño, J. Covas, A. Gomes, L. Gurriana, R. Machado, T. Martins, P. Mendes, R. Pedro, B. Pereira, A. Pontes et al., Nuclear Instruments and Methods in Physics Research Section A: Accelerators, Spectrometers, Detectors and Associated Equipment **1066**, 169627 (2024)

[14] G.S. University, *Hyperphysics: Atmospheric muons, http://www.hyperphysics.phy-astr.gsu.edu/hbase/particles/muonatm.html (accessed: 26/06/2025)*